Jundishapur J Nat Pharm Prod. 2022 August; 17(3):e120271. https://doi.org/10.5812/jjnpp.120271.

Published online 2022 January 3. **Research Article**

Explanation of Structure and Function of kv1.3 Potent Blocker from *Mesobuthus eupeus* Venom Gland: A New Promise in Drug Development

Mohammad Javad Khodayar [1, 2], Masoud Mahdavinia [1, 2], Masoumeh Baradaran [1, *] and Amir Jalali [3]

[1] Toxicology Research Center, Medical Basic Sciences Research Institute, Ahvaz Jundishapur University of Medical Sciences, Ahvaz, Iran
[2] Department of Toxicology, School of Pharmacy, Ahvaz Jundishapur University of Medical Sciences, Ahvaz, Iran
[3] Department of Operating Room, Langroud School of Allied Medical Sciences, Guilan University of Medical Sciences, Rasht, Iran

[*] *Corresponding author*: Toxicology Research Center, Medical Basic Sciences Research Institute, Ahvaz Jundishapur University of Medical Sciences, Ahvaz, Iran. Email: mb.baradaran@gmail.com

Received 2021 October 18; **Accepted** 2021 December 05.

Abstract

Background: Scorpions and other venomous animals are sought with great concern because venom is a source of novel peptides with exciting features. Some toxins of scorpion venom are effectors of potassium channels. Previous studies strongly support the importance of potassium channel toxins for use as pharmacological tools or potential drugs.
Objectives: Here, a three-dimensional (3-D) structure and function of a potent acidic blocker of the human voltage-gated potassium ion channel, Kv1.3, previously identified in the scorpion *Mesobuthus eupeus* venom gland, were interpreted.
Methods: The 3-D structure of meuK2-2 was generated using homology modeling. The interaction of meuK2-2 with the Kv1.3 channel was evaluated using a computational protocol employing peptide-protein docking experiments, pose clustering, and 100 ns molecular dynamic simulations to make the 3-D models of the meuK2-2/Kv1.3 complex trustworthy.
Results: A CSα/β (cysteine-stabilized α-helical and β-sheet) fold was found for the 3-D structure of meuK2-2. In a different mechanism from what was identified so far, meuK2-2 binds to both turret and pore loop of Kv1.3 through two key residues (Ala28 and Ser11) and H-bonds. The binding of meuK2-2 induces some conformational changes to Kv1.3. Eventually, the side chain of a positively charged amino acid (His9) occupies the channel's pore. All together blocks the ion permeation pathway.
Conclusions: MeuK2-2 could block Kv1.3 by a new mechanism. So, it could be a unique target for further investigations to develop a pharmacological tool and potential drug.

Keywords: Scorpion Toxin, meuK2-2, Venom Informatics, Potent Drug, Turret Blocking, Pore Blocking

1. Background

Voltage-gated potassium channels (Kv) are a significant and very varied group of potassium channels, characterized by 12 families (Kv1 to Kv12) (1). The Kv channels have an essential effect on generating and propagating the action potential by detecting fluctuations in transmembrane voltage and linking this detection to channel opening and closing that controls the efflux and influx of K+ ions into the cells (2). The Kv channels are tetrameric transmembrane proteins in which every subunit comprises a membrane-spanning and three extracellular parts. The membrane-spanning part consists of six helical segments (S1 to S6), and the extracellular parts involve the S1-S2 linker, the S3-S4 linker, and the pore region. The pore region includes the pore helix, pore loop, and turret (Figure 1). The S1-S4 linkers form the voltage-sensing domain, and S5-S6 form the pore-forming domain. Voltage-sensing domains sense diverse stimuli, and then K+ ions are transported through the pore (3).

Kv1.3 is preferentially expressed in T cells and is crucial for the activation of these immune cells, suggesting that Kv1.3 plays an essential role in autoimmune diseases, Multiple Sclerosis (MS), rheumatoid arthritis (4), type 1 diabetes (5), asthma (6), psoriasis (7), and neuroinflammatory human disorders such as stroke, epilepsy, Alzheimer's disease, and Parkinson's disease (8). Some studies have demonstrated that the blockers of Kv1.3 can selectively inhibit TEM (effector memory T) lymphocyte activation and improve the immunologic damage (4-6). Accordingly, Kv1.3 has been considered a target for treating T cell-mediated autoimmune diseases, and Kv1.3 blockers have great promise for use as immunosuppressant drugs in autoimmune diseases (8).

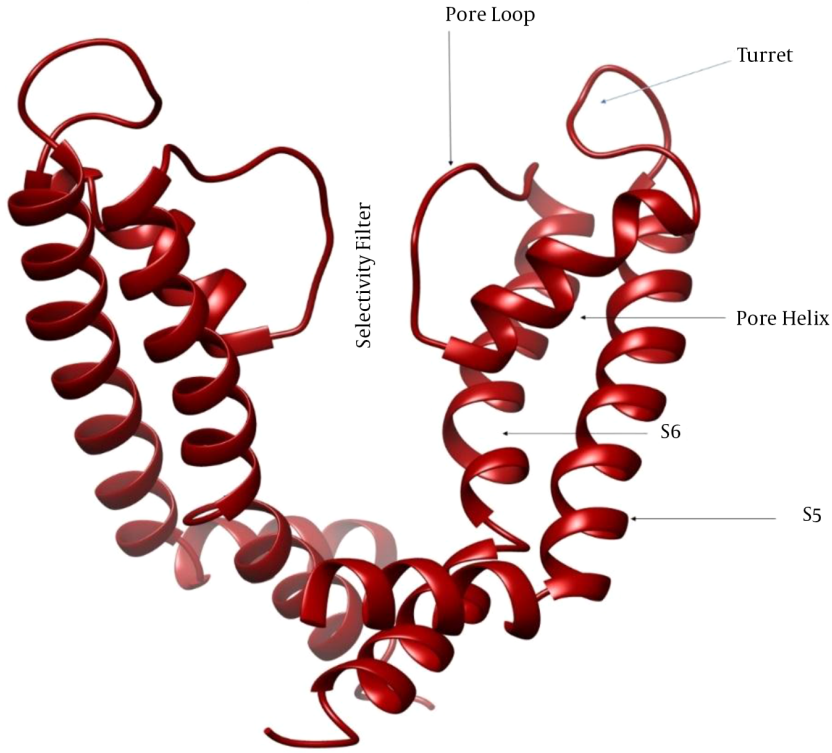

Figure 1. Structure of Kv channels

Scorpion toxins affecting potassium channels (KTxs) represent the potential to apply as valuable tools for developing novel medicines (9). Some peptides derived from scorpion venom are found to block Kv1.3. Up to now, different scorpion Kv1.3 blockers have been characterized, such as OSK1, a toxin from *Orthochirus scrobiculosus* scorpion venom (10), BmP02 (11), BmKTX, and BmKDfsin4 (12) from *Mesobuthus martensii*, Kaliotoxin from *Androctonus mauritanicus* (13), Charybdotoxin from *Leiurus quinquestriatus* (14), maurotoxin from *Scorpio maurus* (15), noxiustoxin from *Centruroides noxius* (16), pi1 toxin from *Pandinus imperator* (17), and Vm24 from *Vaejovis smithi* (18). Among them, ShK derivatives, ShK-186 and ShK-192, are mainly used to treat multiple sclerosis by targeting Kv1.3 channels (8).

Three interaction modes, including gating modifying, pore blocking, and turret blocking, have thoughtfully been described between KTxs and K channels (19). Gating modifier toxins bind to the voltage-sensing domain of K channels and block the channel by changing the closed state stability. Pore-blocking toxins bind at the K channel pore and occlude the ion conduction pathway. Some pore-blocker toxins like agitoxin-2 (20) directly occlude the channel pore with a residue (commonly Lys) occupying the pore of the channel, whereas the others bind to the region far from the central channel pore, i.e., the turret region (21). The exact mechanism by which these toxins block potassium channels remains unclear, while turret block, a general concept whereby the toxin functions as a lid on top of the pore entry, is suggested (19, 21).

Although many KTxs have been characterized from scorpion venom (22), there are still many unknown K+ channel blocker peptides whose identification can be helpful in the world of pharmacology and toxicology research. Moreover, most potassium channels are still in peptide blockers' shortage, and the detection of new KTxs targeting these channels waits for an enormous challenge (23).

2. Objectives

Our study integrated homology modeling, docking analysis, and molecular dynamics simulation to understand the behavior of meuK2-2, a toxin derived from the scorpion *Mesobuthus eupeus* venom gland when exposed to the Kv1.3 channel. Docking analysis and molecular dynamics simulations determined the binding regions of meuk2-2 to Kv1.3 and identified residues involved in the interaction. The findings could suggest a new mechanism for meuK2-2 as a blocker of Kv1.3.

3. Methods

3.1. cDNA Library Construction and Screening

The cDNA library was constructed from the Iranian *M. eupeus* venom gland as described previously (24). Clones carrying a DNA insert of more than 700 base pairs, which theoretically can encode venom peptide precursors, were selected for cDNA sequencing. We deposited the nucleotide sequence applied in the current study in the GenBank database (http://www.ncbi.nlm.nih.gov) under accession number KU253401 (referred to as meuK2-2). By searching the GenBank database, BLASTP (https://blast.ncbi.nlm.nih.gov/Blast.cgi?PAGE = Proteins) uncovered that the homologs of meuK2-2 are mostly potent blockers of Kv1.3. The molecular weight and Isoelectric Point (IP) of meuK2-2 were calculated using the proteomics tool from the INNOVAGEN server (http://www.innovagen.com/proteomics-tools).

3.2. Generation and Refinement of Three-Dimensional Structures

The three-dimensional structures of the newly obtained KTx, meuK2-2, and KV1.3 were provided by program MODELLER (25) using homology-based protein structure models. A search against the Protein Data Bank Proteins (PDB) database was done to find the most similar structures to meuK2-2 and Kv1.3. The most similar peptide/protein with more than 75% identity was selected for homology modeling. Besides, BmP03 (PDB ID: 1WM8) and Kv1.2 (PDB ID: 5WIE) were selected as templates for modeling meuK2-2 and KV1.3, respectively. Following the modeling process with MODELLER, we selected the best model based on parameters, such as the smallest DOPE assessment score and the highest GA341 assessment score.

3.3. Molecular Docking of meuK2-2 with Kv1.3 Channel

Software HADDOCK (26) was used to investigate how the meuK2-2 interacts with the Kv1.3 channel. This program performs protein-protein docking using the molecular dynamics simulation technique entirely flexibly. Next, the residues playing a direct role in the toxin and potassium channel interaction were determined. These residues are defined as Ambiguous Interaction Restraints (AIR). Ambiguous interaction restraints are employed for molecular docking and defined through a list of residues that fall under two categories: active and passive. In general, active residues are of central importance for interaction. These active residues throughout the simulation must be part of the interface; otherwise, they will be penalized for scoring. Passive residues are those contributing to the interaction but are deemed of less importance.

After molecular docking, intermolecular interaction energy is used to rank the docking results. This energy is the sum of electrostatic and van der Waals energies. In HADDOCK software, amino acids with a direct effect on the interaction are called active amino acids, and the amino acids around the active amino acids are called passive amino acids. Amino acids with a water exposure level greater than 50% are considered active amino acids (26). Here, all ligand residues and amino acids in the pore of the Kv1.3 channel were defined as active amino acids. In the first cluster of docking results, the most regular conformation was selected to evaluate the complex stability by molecular dynamics simulation.

3.4. Molecular Dynamics Simulation

To evaluate the binding interaction between meuK2-2 and Kv1.3, we simulated the meuK2-2/Kv1.3 complex using a protein-water system in the NVT ensemble by Gromacs 2019.6 (27). Before the simulation, the CHARMM-GUI server (28) placed the meuK2-2/Kv1.3 complex inside the phospholipid membrane and prepared input files for simulation. Phosphatidylcholine (POPC) was used to make the phospholipid membrane. A total of 262 POPCs were applied for two layers of the phospholipid membrane. To balance the net charge of the system, we added Na+ and Cl- ions to the simulation box to 150 mM. The steepest descent algorithm was used for energy minimization. While running the simulation, the temperature and pressure were made constant using the Berendsen algorithm at 310 K and 1 atm, respectively. Finally, the ultimate complex simulation was run with the help of Gromacs 2019.6 with a time step of 2 fs for 100 ns (50 million steps). The PME algorithm was applied to calculate the electrostatic interactions. The SHAKE algorithm was developed to keep the length of the covalent bonds constant.

The software VMD was applied to visualize the trajectories and perform analyses. To evaluate the stability of the peptide in the binding region on the Kv1.3 channel, we measured the root-mean-square deviation (RMSD) (29). The RMSD changes related to alpha carbon atoms of ligand were calculated during the running time of simulation relative to the original structure. Finally, RMSD was used to evaluate the stability of meuK2-2 at the binding site on the Kv1.3 channel. The structure of the meuK2-2/Kv1.3 complex before and after simulation was visualized and compared with a molecular visualization program, UCSF ChimeraX (30).

4. Results

4.1. Characterization and Modeling of meuK2-2

MeuK2-2 is a 28-amino acid peptide with molecular weight and IP of 2884 Dalton and 4.42, respectively. Based on IP, meuK2-2 is an acidic peptide. Sequence alignment demonstrated that meuK2-2 had extensive homology with

α-KTx9 subfamily members (Figure 2A). The meuK2-2 final 3-D structure is shown in Figure 2B. As shown, meuK2-2 contains six Cys residues forming three disulfide bridges, and presents two structural domains: one α-helix and a double-stranded beta-sheet, indicating that they adopt a CS$\alpha\beta$ (cysteine-stabilized α-helical and β-sheet) folding. The structure of CS$\alpha\beta$ is created from a single α-helix connecting to a double or triple stranded β-sheet employing three or four disulfide bonds (31). Two random coils were also detected in the structure of meuK2-2.

4.2. meuK2-2/Kv1.3 Interaction

The modeled meuK2-2 was docked with Kv1.3 to generate their binding mode. The results of the docking are shown in Table 1. The binding energy between Kv1.3 and meuK2-2 of the first four clusters accompanied by the member number of each cluster is shown in this table. Cluster 1 has 16 members and the most significant number of the structures, but it shows the weakest interaction among the other three clusters in terms of energy. Due to the slight difference in the number of members related to clusters 1 and 2, cluster 2 was used to study the molecular dynamics and evaluate the stability of meuK2-2 in the binding region.

Table 1. Connection Scores and Cluster Sizes in the First Four Clusters Obtained from Molecular Docking

Cluster	HADDOCK Score	Cluster Size
1	-20.193	16
2	-65.92	12
3	-43.130	10
4	-63.505	10

The interacting amino acids in the docking of meuK2-2 towards Kv1.3 are shown in Figure 3A. Nine residues of meuK2-2 (Val1, Lys8, His9, Lys13, Asp21, Cys24, Asn25, Cys26, and Ala28) were found to involve in interactions with 10 residues (Ser328, Tyr349, Asp351, His353, Tyr742, His749, Ser117, Gly1136, Asp1137, and Asp1504) on the surface of the vestibule of Kv1.3 channel through H-bonds.

The 3-D view of meuk2-2, when docked with Kv1.3, is illustrated in Figure 3B. As shown in Figure 4C, after the interaction of the meuk2-2 with the amino acids on the surface of Kv1.3, His9 entered directly into the channel's pore. So, it could block the channel.

4.3. Structural Stability Analysis Upon meuK2-2 Binding Using MD Simulation

We calculated the RMSD changes of meuK2-2 to analyze meuK2-2 behavior during simulation. As a general rule, RMSD values reflect the local flexibility and mobility of the protein during MD simulation. So, a greater residue RMSD value indicates greater mobility and vice versa. We calculated the RMSD values for meuk2-2 using MD simulation. The results are shown in Figure 4. At the beginning of the simulation, the RMSD chart shows a slight upward trend, and this increase lasts up to 50,000 ps so that at this time, the RMSD value is equal to about 0.18 nm. From this time to the end of the simulation, the RMSD value remains constant at 0.18 nm, indicating the peptide structure's stability in the binding region after the time of 50,000 ps.

Figure 5 shows the conformational changes of meuK2-2 after simulation. According to this figure, the peptide binding conformation is shifted after simulation, and some interactions between the peptide and the channel are lost. The peptide, however, still retains its binding to the channel via three residues (His9, Ser11, and Ala28). After simulation, Ala28, in addition to Ser328, reacts with Ser172 of the channel, and His9 reacts with Asp351 instead of Tyr349. Moreover, Ser11, which had not participated in the reaction before simulation, enters the reaction with Asp351 after simulation. The interesting point is the location of His9, which penetrated the channel's pore in both cases before and after simulation (Figure 5C).

A better illustration of the hypothesized model of meuK2-2/Kv1.3 interaction and conformational changes of Kv1.3 induced by meuK2-2 is shown in Figure 6. As shown, Ala28 was bound to the turret region and Ser11 to pore the loop. The binding of Ala28 to the turret bent it inward close to the pore entry. His9 occluded the pore, and other parts of meuK2-2 acted as a lid above the pore entry. Moreover, the selectivity filter of Kv1.3 was tightened due to binding meuK2-2 to the channel.

5. Discussion

Some research has proved the effects of scorpion KTxs on some potassium channels consisting of SKCa, Kv1.x, BKCa, Kv11.1, and IKCa (24, 25). However, new KTx inhibitors are required for channel structure-function studies as potential drugs for the treatment of potassium channel-related disorders for which an inhibitor does not exist (25). Basic scorpion KTxs have been extensively employed in studies of toxin/potassium channel interaction assays. However, research on acidic KTxs has been progressed slowly (32). The findings of the current study show how an acidic peptide, meuK2-2, derived from the scorpion M. eupeus venom, can be an effector of the potassium channel Kv1.3. To produce a trustworthy 3-D model of the meuK2-2/ Kv1.3 complex, a computational protocol employing homology modeling, followed by molecular docking experiments, pose clustering, and molecular dynamic simulations (100 ns), was developed. The results showed that meuK2-2 has a modified CS$\alpha\beta$ structure, and when it encounters the Kv1.3 channel, it interacts with the residues

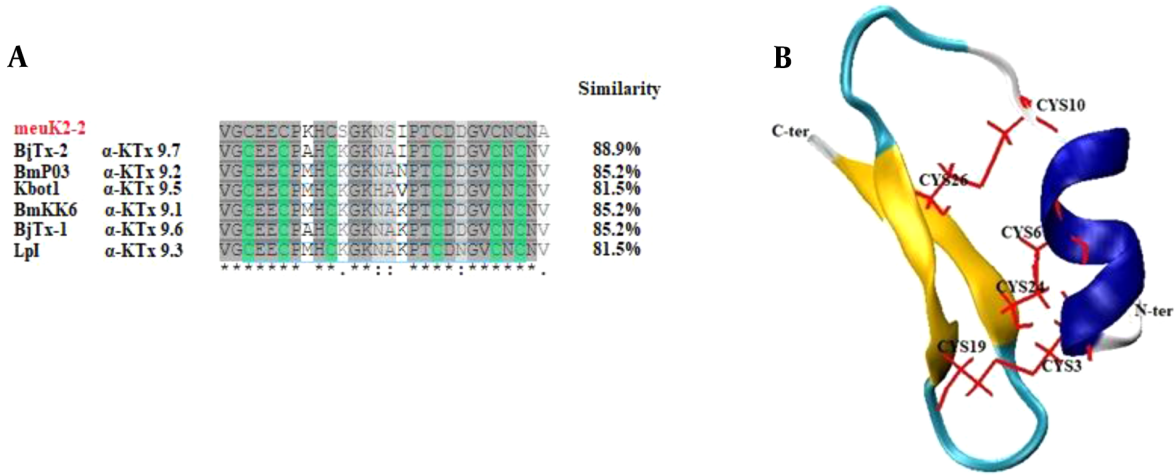

Figure 2. A, multiple sequence alignment of meuK2-2 with other α-KTx9 members; B, 3-D view of the modeled meuK2-2. Disulfide bonds (red lines) connect the β-sheet (yellow) to the alpha-helix (dark blue), facilitating the folding of the peptide into a CS$\alpha\beta$ structure. Random coils are shown in light blue.

of the turret and pore loop of Kv1.3; eventually, His9 penetrates the pore of the channel and blocks the ion permeation pathway. Moreover, the position of meuK2-2 as a lid above the Kv1.3 helps block the channel.

The vast majority of scorpion venom peptides are basic. However, a few anionic peptides with no toxicity properties have previously been characterized from the venom gland of *Mesobuthus martensii* [BmKa1, BmKa2 (33), and HAP-1 (34)], *Tityus costatus* (four peptides) (35), *Scorpiops jendeki* (SJE098.1 and SJE098.2) (35), *Buthus occitanus Israelis* (BoiTx776 from) (36), *Hottentotta judaicus* (HjVP) (37), and *Androctonus bicolor* (38). The function of most of these peptides has not yet been characterized. It was previously thought that these peptides only play a part in balancing the pH of scorpion venom liquid (33). However, Shi et al. recently showed that HAP-1 has an inhibitory effect on the antimicrobial peptide activity of M. martensii Karsch venom (34). Now, acidic peptides are known as a new class of scorpion peptides characterized by (1) IP < 5.0; (2) being highly hydrophilic; and (3) having random coil regions and some α-helical domains (34). Due to IP (4.42), the presence of random coil, and α-helical domains in the 3-D structure, meuK2-2 is an acidic toxin that can make it unique as a toxic KTx. This peptide appears to be a bifunctional peptide with two roles in the venom gland of M. eupeus, blocking the K channel and balancing the pH of the venom liquid.

The homology modeling of meuK2-2 revealed a CS$\alpha\beta$ folding. Peptides with the CS$\alpha\beta$ structure are the most predominant components of scorpion venom-affecting potassium channels (39). A study using the molecular evolutionary analysis showed that most CSα/β toxin scaffolds underwent the periodic effect of positive selection, compared to non-CSα/β linear toxins (40). KTxs are structurally classified into seven different groups, i.e., α, β, γ, κ, δ, λ, and ε-KTx. Seven different scaffold motifs have been identified within the structure of scorpion toxins: CS-α/β, CS-α/α, ICK (inhibitor cystine knot), DDH (disulfide-directed β-hairpin), Kunitz-type structural fold with a double-stranded antiparallel β-sheet flanked by an α-helix, and a knotting type fold, stabilized by four disulfide bridges (41). The CSα/β motif occurs in α-, β-, and γ-KTxs subfamilies (39). MeuK2-2 was also classified as an α-KTx, confirmed by the presence of the CSα/β motif in its structure.

In one classification, scorpion toxins were classified into six main groups and 16 subgroups, based on both functional and structural characteristics (40). The CSα/β toxins were classified as the leading group with six subgroups, including CS$\alpha\beta$'alpha, CS$\alpha\beta$'beta, CS$\alpha\beta$'chlorotoxin, CS$\alpha\beta$'lipo, CS$\alpha\beta$'scorpine, CS$\alpha\beta$'long-chain, and CS$\alpha\beta$'short-chain. Only the last three subgroups affect the potassium channels (40). Excluding CS$\alpha\beta$'scorpine', which contains β-KTxs, meuK2-2 is classified in the CS$\alpha\beta$'short-chain' group because of its short length (28 amino acids).

Mutagenesis and computational experiments have suggested various interactions between potassium channels and scorpion toxins (24). Our docking experiments determined that meuK2-2, like charybdotoxin (42), is a pore blocker toxin that binds to the pore loop through a residue (Ser11), and like ErgTx1 (43) and Cs1 (19), two turret blocker toxins, binds to the turret through a hydrophobic residue (Ala28). Unlike Charybdotoxin that blocks the channel by entering the side chain of Lys residue in the pore, meuK2-

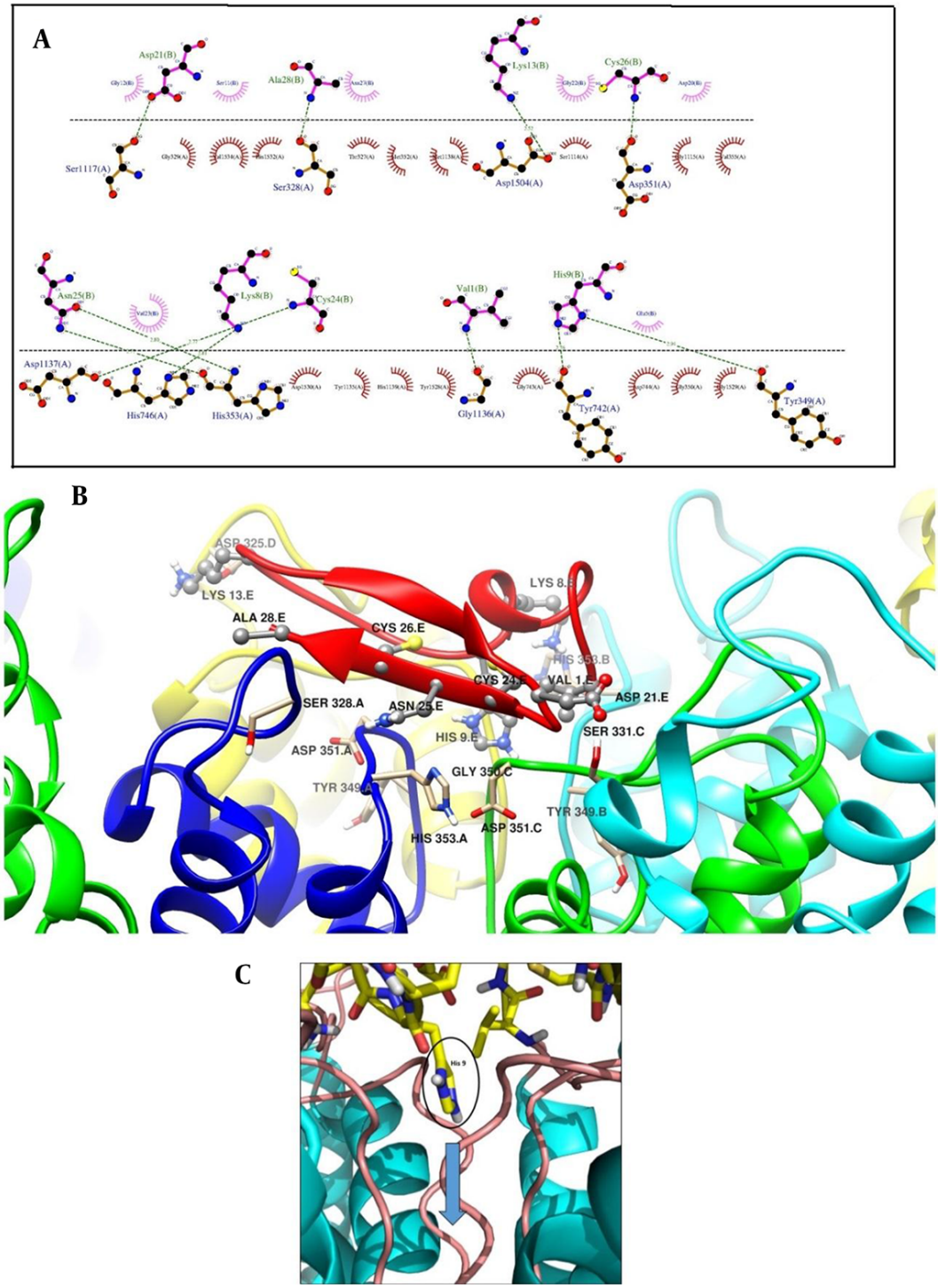

Figure 3. A, the interaction of meuK2-2 with the Kv1.3 channel with possible H-bonds resulting from docking. The dashed lines represent H-bond interactions. Critical residues of meuK2-2 are shown in pink color and crucial residues of Kv1.3 in orange color; B, 3-D presentation of meuK2-2 (red color) and Kv1.3 interactions. Residues of meuK2-2 and Kv1.3 contribute to the interaction; C, Kv1.3 channel blockade with the entry of residue His9. The pore path is indicated by a blue arrow.

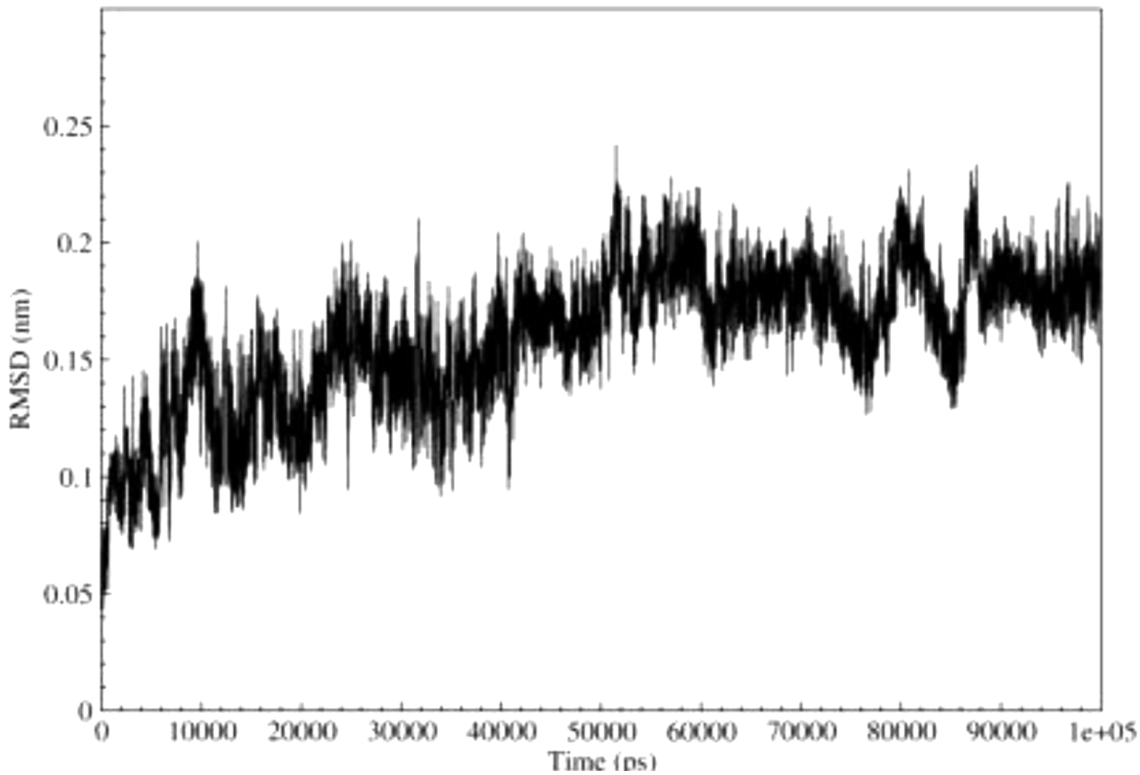

Figure 4. Diagram of RMSD changes of meuK2-2 during molecular dynamics simulation (100 ns)

2 occludes the pore with the His residue. Both Lys and His are classified in amino acids with positively charged side chains.

The importance of hydrophobic side chains in the stable binding of potassium channel blockers has previously been identified. Leneaus et al. demonstrated that hydrophobic side chains stabilize the binding of quaternary ammonium (QA) compounds (potassium channel blockers) to the surface of the potassium channel cavity (44). Therefore, the hydrophobic interaction between meuK2-2 and Kv1.3 through Ala28 and Ser172 could play an essential role in stabilizing the meuK2-2/ Kv1.3 complex.

Some scorpion toxins like charybdotoxin did not induce conformational changes in binding to potassium channels (42), while noticeable conformational changes were induced by some other scorpion toxins like kaliotoxin (45) and ADWX-1 (46). Conformational changes predominantly occur in potassium channels' channel turret or filter region upon different scorpion toxin bindings (47). Computational simulations revealed that during the binding of ADWX-1 toxin to the Kv1.3 channel, the channel turret from one Kv1.3 chain makes close contact with ADWX-1 toxin, while the rest of the chains bend outward and move away from the ADWX-1 toxin (46). These findings are in line with what was found here for meuK2-2. When meuK2-2 associates with the Kv1.3 channel, it binds to the turret and bends it inward close to the pore entry (Figure 6).

In contrast to ADWX-1, the selectivity filter plays a vital role in binding the Kv1.3 channel to the scorpion toxin, maurotoxin. During the binding of maurotoxin to the Kv1.3 channel, conformational changes were induced in the channel filter region rather than the channel turret (48). MeuK2-2, in addition to the turret channel, binds to the pore loop simultaneously. The binding of meuK2-2 to the pore loop induces conformational changes, leading to the selectivity filter getting tighter (Figure 6).

In an overall comparison, meuK2-2 behaves somewhat like pore blocker toxins and somewhat like turret blocker toxins. Pore blocker toxins plug the K+ ion conduction pathway by entering a residue in the channel pore, whereas turret blockers locate as a lid at the pore entry and prevent K+ ions currents (21). MeuK2-2 has both features in the interaction with Kv1.3. Moreover, a tighter selectivity filter results from the meuK2-2/ Kv1.3 interactions. We propose it as a new mechanism of scorpion toxins (or pos-

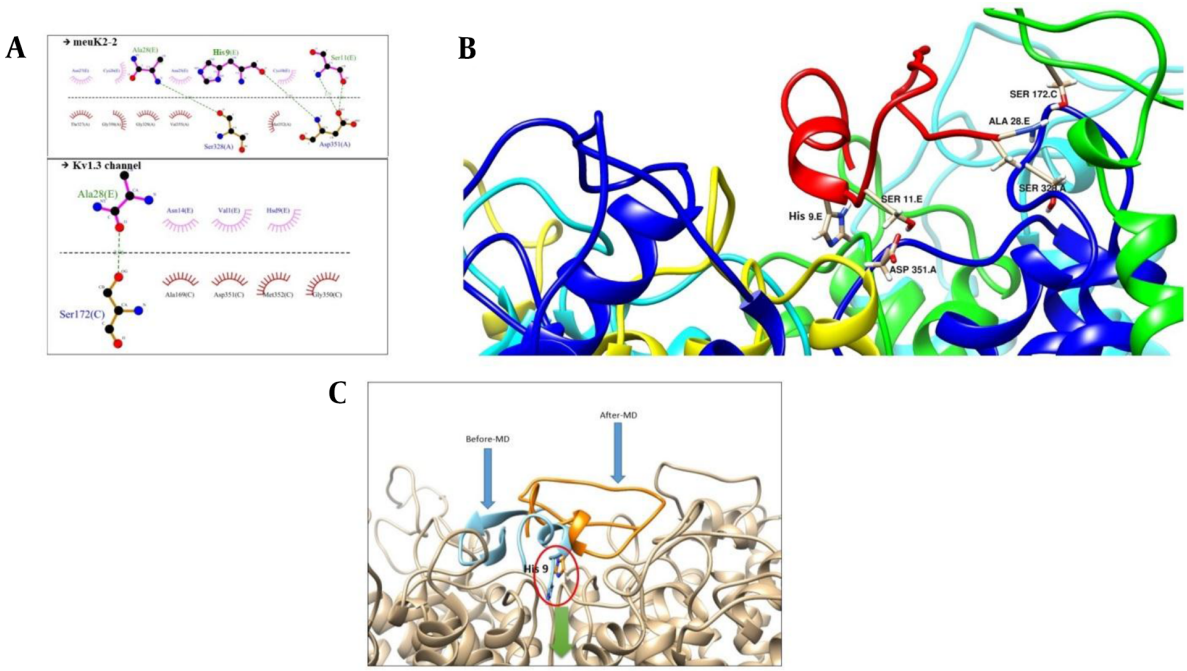

Figure 5. A, crucial residues in the interaction of meuK2-2 to Kv1.3 after simulation; B, 3-D view of participating residues in the meuK2-2/Kv1.3 interactions. meuK2-2 is in red; C, conformational changes of meuK2-2 in the binding mode on the vestibule of Kv1.3, before (blue) and after MD-simulation (orange). The green arrow indicates the channel pore. Note the position of His9, before and after MD simulation.

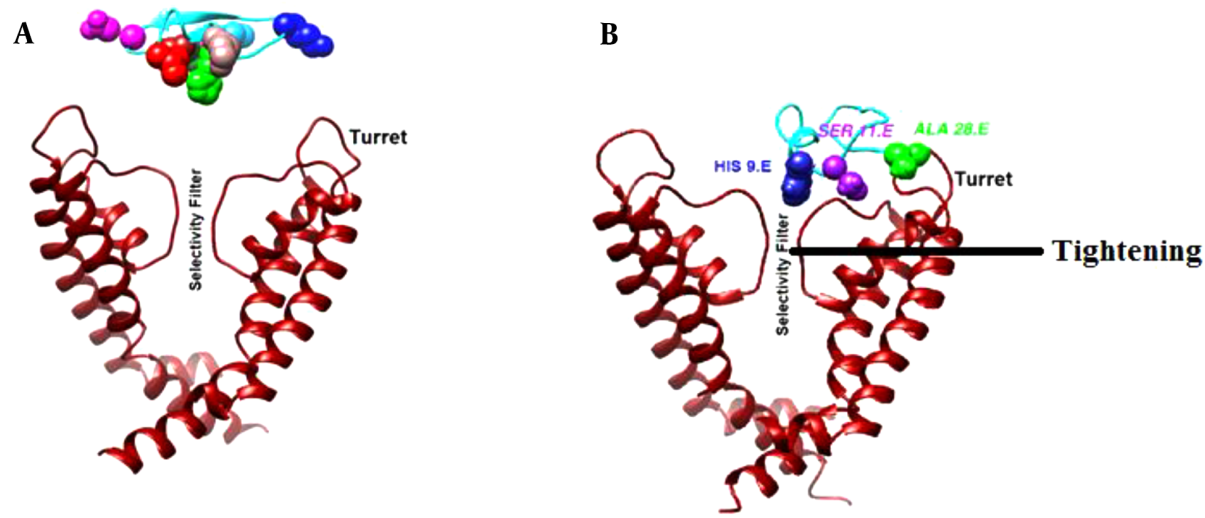

Figure 6. Conformation changes of Kv1.3, induced by meuK2-2. A, before binding of meuK2-2; B, after binding of meuK2-2. The turret has bent inward close to the pore entry, the selectivity filter has become tighter, His9 has penetrated the pore, and other parts of meuK2-2 act as a lid above the pore entry.

sibly basic scorpion toxins) and potassium channels interactions. Further research can shed new light on meuK2-2/Kv1.3 interactions.

The Kv channel blockers are known to be new tools to inhibit the activation of T-cells, resulting in specific immunosuppression. Besides, Kv1.3 is the primary channel on human effector memory T lymphocytes; consequently, it composes an appealing pharmacological target for au-

toimmune diseases mediated by T cell immunomodulation (49). Functional characterization of meuK2-2 as a potent Kv1.3-targeted peptide will create new therapeutic agents for human autoimmune diseases.

Acknowledgments

The authors would like to express their gratitude to Ahvaz Jundishapur University of Medical Sciences for financial support (grant number: TRC0008). We are also immensely grateful to Iman Ivaz for his comments on an earlier manuscript version.

Footnotes

Authors' Contribution: M. B. participated in research design, conducted experiments, performed data analysis, and wrote the manuscript. MJ. K. conducted data analysis and contributed to the writing of the manuscript. M. M. was responsible for some computational analysis and contributed to manuscript revision. A.J revised the manuscript.

Conflict of Interests: The authors declare that they have no known competing financial interests or personal relationships that could have influenced the work reported in this paper.

Ethical Approval: All research steps were done after obtaining ethical approval from the Research Ethics Committee (approval number: IR.AJUMS.REC.1400.146).

Funding/Support: This study was supported by grant TRC-0008 from the Jundishapur University of Medical Sciences, Ahvaz, Iran.

References

1. Yang S, Jan LY. Potassium Channels: Their Physiological and Molecular Diversity. In: Roberts GC, editor. *Encyclopedia of Biophysics*. Heidelberg, Germany: Springer; 2013. p. 1933–41. https://doi.org/10.1007/978-3-642-16712-6_358.
2. Grizel AV, Glukhov GS, Sokolova OS. Mechanisms of activation of voltage-gated potassium channels. *Acta Naturae*. 2014;**6**(4):10–26. [PubMed: 25558391]. [PubMed Central: PMC4273088].
3. Kuang Q, Purhonen P, Hebert H. Structure of potassium channels. *Cell Mol Life Sci*. 2015;**72**(19):3677–93. [PubMed: 26070303]. [PubMed Central: PMC4565861]. https://doi.org/10.1007/s00018-015-1948-5.
4. Fasth AE, Cao D, van Vollenhoven R, Trollmo C, Malmstrom V. CD28nullCD4+ T cells-characterization of an effector memory T-cell population in patients with rheumatoid arthritis. *Scand J Immunol*. 2004;**60**(1-2):199–208. [PubMed: 15238090]. https://doi.org/10.1111/j.0300-9475.2004.01464.x.
5. Viglietta V, Kent SC, Orban T, Hafler DA. GAD65-reactive T cells are activated in patients with autoimmune type 1a diabetes. *J Clin Invest*. 2002;**109**(7):895–903. [PubMed: 11927616]. [PubMed Central: PMC150925]. https://doi.org/10.1172/JCI14114.
6. Koshy S, Huq R, Tanner MR, Atik MA, Porter PC, Khan FS, et al. Blocking KV1.3 channels inhibits Th2 lymphocyte function and treats a rat model of asthma. *J Biol Chem*. 2014;**289**(18):12623–32. [PubMed: 24644290]. [PubMed Central: PMC4007452]. https://doi.org/10.1074/jbc.M113.517037.
7. Nguyen W, Howard BL, Neale DS, Thompson PE, White PJ, Wulff H, et al. Use of Kv1.3 blockers for inflammatory skin conditions. *Curr Med Chem*. 2010;**17**(26):2882–96. [PubMed: 20858170]. [PubMed Central: PMC3337760]. https://doi.org/10.2174/092986710792065072.
8. Wang X, Li G, Guo J, Zhang Z, Zhang S, Zhu Y, et al. Kv1.3 Channel as a Key Therapeutic Target for Neuroinflammatory Diseases: State of the Art and Beyond. *Front Neurosci*. 2019;**13**:1393. [PubMed: 31992966]. [PubMed Central: PMC6971160]. https://doi.org/10.3389/fnins.2019.01393.
9. Beeton C, Wulff H, Barbaria J, Clot-Faybesse O, Pennington M, Bernard D, et al. Selective blockade of T lymphocyte K(+) channels ameliorates experimental autoimmune encephalomyelitis, a model for multiple sclerosis. *Proc Natl Acad Sci U S A*. 2001;**98**(24):13942–7. [PubMed: 11717451]. [PubMed Central: PMC61146]. https://doi.org/10.1073/pnas.241497298.
10. Tegla CA, Cudrici C, Rozycka M, Soloviova K, Ito T, Singh AK, et al. C5b-9-activated, K(v)1.3 channels mediate oligodendrocyte cell cycle activation and dedifferentiation. *Exp Mol Pathol*. 2011;**91**(1):335–45. [PubMed: 21540025]. [PubMed Central: PMC3139709]. https://doi.org/10.1016/j.yexmp.2011.04.006.
11. Wu B, Wu BF, Feng YJ, Tao J, Ji YH. Mapping the Interaction Anatomy of BmP02 on Kv1.3 Channel. *Sci Rep*. 2016;**6**:29431. [PubMed: 27403813]. [PubMed Central: PMC4941521]. https://doi.org/10.1038/srep29431.
12. Meng L, Xie Z, Zhang Q, Li Y, Yang F, Chen Z, et al. Scorpion Potassium Channel-blocking Defensin Highlights a Functional Link with Neurotoxin. *J Biol Chem*. 2016;**291**(13):7097–106. [PubMed: 26817841]. [PubMed Central: PMC4807291]. https://doi.org/10.1074/jbc.M115.680611.
13. Gairi M, Romi R, Fernandez I, Rochat H, Martin-Eauclaire MF, Van Rietschoten J, et al. 3D structure of kaliotoxin: is residue 34 a key for channel selectivity? *J Pept Sci*. 1997;**3**(4):314–9. [PubMed: 9262650]. https://doi.org/10.1002/(SICI)1099-1387(199707)3:4%3C314::AID-PSC117%3E3.0.CO;2-E.
14. Hu L, Pennington M, Jiang Q, Whartenby KA, Calabresi PA. Characterization of the functional properties of the voltage-gated potassium channel Kv1.3 in human CD4+ T lymphocytes. *J Immunol*. 2007;**179**(7):4563–70. [PubMed: 17878353]. https://doi.org/10.4049/jimmunol.179.7.4563.
15. Jensen BS, Hertz M, Christophersen P, Madsen LS. The Ca2+-activated K+ channel of intermediate conductance:a possible target for immune suppression. *Expert Opin Ther Targets*. 2002;**6**(6):623–36. [PubMed: 12472376]. https://doi.org/10.1517/14728222.6.6.623.
16. Sitges M, Possani LD, Bayon A. Noxiustoxin, a short-chain toxin from the Mexican scorpion Centruroides noxius, induces transmitter release by blocking K+ permeability. *J Neurosci*. 1986;**6**(6):1570–4. [PubMed: 3012016]. [PubMed Central: PMC6568734].
17. Peter MJ, Hajdu P, Varga Z, Damjanovich S, Possani LD, Panyi G, et al. Blockage of human T lymphocyte Kv1.3 channels by Pi1, a novel class of scorpion toxin. *Biochem Biophys Res Commun*. 2000;**278**(1):34–7. [PubMed: 11071851]. https://doi.org/10.1006/bbrc.2000.3756.
18. Gurrola GB, Hernandez-Lopez RA, Rodriguez de la Vega RC, Varga Z, Batista CV, Salas-Castillo SP, et al. Structure, function, and chemical synthesis of Vaejovis mexicanus peptide 24: a novel potent blocker of Kv1.3 potassium channels of human T lymphocytes. *Biochemistry*. 2012;**51**(19):4049–61. [PubMed: 22540187]. https://doi.org/10.1021/bi300060n.
19. Karbat I, Altman-Gueta H, Fine S, Szanto T, Hamer-Rogotner S, Dym O, et al. Pore-modulating toxins exploit inherent slow inactivation to block K(+) channels. *Proc Natl Acad Sci U S A*. 2019;**116**(37):18700–9. [PubMed: 31444298]. [PubMed Central: PMC6744907]. https://doi.org/10.1073/pnas.1908903116.
20. Ranganathan R, Lewis JH, MacKinnon R. Spatial localization of the K+ channel selectivity filter by mutant cycle-based structure analysis. *Neuron*. 1996;**16**(1):131–9. [PubMed: 8562077]. https://doi.org/10.1016/s0896-6273(00)80030-6.

21. Xu CQ, Zhu SY, Chi CW, Tytgat J. Turret and pore block of K+ channels: what is the difference? *Trends Pharmacol Sci*. 2003;**24**(9):446–8. author reply 448-9. [PubMed: 12967767]. https://doi.org/10.1016/S0165-6147(03)00223-2.
22. Kuzmenkov AI, Vassilevski AA, Kudryashova KS, Nekrasova OV, Peigneur S, Tytgat J, et al. Variability of Potassium Channel Blockers in Mesobuthus eupeus Scorpion Venom with Focus on Kv1.1: AN INTEGRATED TRANSCRIPTOMIC AND PROTEOMIC STUDY. *J Biol Chem*. 2015;**290**(19):12195–209. [PubMed: 25792741]. [PubMed Central: PMC4424352]. https://doi.org/10.1074/jbc.M115.637611.
23. Ramu Y, Xu Y, Lu Z. Engineered specific and high-affinity inhibitor for a subtype of inward-rectifier K+ channels. *Proc Natl Acad Sci U S A*. 2008;**105**(31):10774–8. [PubMed: 18669667]. [PubMed Central: PMC2504780]. https://doi.org/10.1073/pnas.0802850105.
24. Baradaran M, Jalali A, Naderi-Soorki M, Jokar M, Galehdari H. First Transcriptome Analysis of Iranian Scorpion, Mesobuthus Eupeus Venom Gland. *Iran J Pharm Res*. 2018;**17**(4):1488–502. [PubMed: 30568706]. [PubMed Central: PMC6269579].
25. Webb B, Sali A. Comparative Protein Structure Modeling Using MODELLER. *Curr Protoc Bioinformatics*. 2016;**54**:5 6 1–5 6 37. [PubMed: 27322406]. [PubMed Central: PMC5031415]. https://doi.org/10.1002/cpbi.3.
26. de Vries SJ, van Dijk M, Bonvin AM. The HADDOCK web server for data-driven biomolecular docking. *Nat Protoc*. 2010;**5**(5):883–97. [PubMed: 20431534]. https://doi.org/10.1038/nprot.2010.32.
27. GROMACS Development Team. *GROMACS Documentation 2019.6*. Sweeden: GROMACS; 2020.
28. Jo S, Kim T, Iyer VG, Im W. CHARMM-GUI: a web-based graphical user interface for CHARMM. *J Comput Chem*. 2008;**29**(11):1859–65. [PubMed: 18351591]. https://doi.org/10.1002/jcc.20945.
29. Sargsyan K, Grauffel C, Lim C. How Molecular Size Impacts RMSD Applications in Molecular Dynamics Simulations. *J Chem Theory Comput*. 2017;**13**(4):1518–24. [PubMed: 28267328]. https://doi.org/10.1021/acs.jctc.7b00028.
30. Pettersen EF, Goddard TD, Huang CC, Couch GS, Greenblatt DM, Meng EC, et al. UCSF Chimera–a visualization system for exploratory research and analysis. *J Comput Chem*. 2004;**25**(13):1605–12. [PubMed: 15264254]. https://doi.org/10.1002/jcc.20084.
31. Saucedo AL, Flores-Solis D, Rodriguez de la Vega RC, Ramirez-Cordero B, Hernandez-Lopez R, Cano-Sanchez P, et al. New tricks of an old pattern: structural versatility of scorpion toxins with common cysteine spacing. *J Biol Chem*. 2012;**287**(15):12321–30. [PubMed: 22238341]. [PubMed Central: PMC3320981]. https://doi.org/10.1074/jbc.M111.329607.
32. Chen ZY, Zeng DY, Hu YT, He YW, Pan N, Ding JP, et al. Structural and functional diversity of acidic scorpion potassium channel toxins. *PLoS One*. 2012;**7**(4). e35154. [PubMed: 22511981]. [PubMed Central: PMC3325286]. https://doi.org/10.1371/journal.pone.0035154.
33. Zeng XC, Wang SX, Zhu Y, Zhu SY, Li WX. Identification and functional characterization of novel scorpion venom peptides with no disulfide bridge from Buthus martensii Karsch. *Peptides*. 2004;**25**(2):143–50. [PubMed: 15062994]. https://doi.org/10.1016/j.peptides.2003.12.003.
34. Shi W, He P, Zeng XC, Wu W, Chen X. Inhibitory Effect of an Acidic Peptide on the Activity of an Antimicrobial Peptide from the Scorpion Mesobuthus martensii Karsch. *Molecules*. 2018;**23**(12). [PubMed: 30558111]. [PubMed Central: PMC6321396]. https://doi.org/10.3390/molecules23123314.
35. Diego-Garcia E, Batista CV, Garcia-Gomez BI, Lucas S, Candido DM, Gomez-Lagunas F, et al. The Brazilian scorpion Tityus costatus Karsch: genes, peptides and function. *Toxicon*. 2005;**45**(3):273–83. [PubMed: 15683865]. https://doi.org/10.1016/j.toxicon.2004.10.014.
36. Kozminsky-Atias A, Bar-Shalom A, Mishmar D, Zilberberg N. Assembling an arsenal, the scorpion way. *BMC Evol Biol*. 2008;**8**:333. [PubMed: 19087317]. [PubMed Central: PMC2651877]. https://doi.org/10.1186/1471-2148-8-333.
37. Morgenstern D, Rohde BH, King GF, Tal T, Sher D, Zlotkin E. The tale of a resting gland: transcriptome of a replete venom gland from the scorpion Hottentotta judaicus. *Toxicon*. 2011;**57**(5):695–703. [PubMed: 21329713]. https://doi.org/10.1016/j.toxicon.2011.02.001.
38. Zhang L, Shi W, Zeng XC, Ge F, Yang M, Nie Y, et al. Unique diversity of the venom peptides from the scorpion Androctonus bicolor revealed by transcriptomic and proteomic analysis. *J Proteomics*. 2015;**128**:231–50. [PubMed: 26254009]. https://doi.org/10.1016/j.jprot.2015.07.030.
39. Gao B, Harvey PJ, Craik DJ, Ronjat M, De Waard M, Zhu S. Functional evolution of scorpion venom peptides with an inhibitor cystine knot fold. *Biosci Rep*. 2013;**33**(3). [PubMed: 23721518]. [PubMed Central: PMC3694633]. https://doi.org/10.1042/BSR20130052.
40. Sunagar K, Undheim EA, Chan AH, Koludarov I, Munoz-Gomez SA, Antunes A, et al. Evolution stings: the origin and diversification of scorpion toxin peptide scaffolds. *Toxins (Basel)*. 2013;**5**(12):2456–87. [PubMed: 24351712]. [PubMed Central: PMC3873696]. https://doi.org/10.3390/toxins5122456.
41. Cremonez CM, Maiti M, Peigneur S, Cassoli JS, Dutra AA, Waelkens E, et al. Structural and Functional Elucidation of Peptide Ts11 Shows Evidence of a Novel Subfamily of Scorpion Venom Toxins. *Toxins (Basel)*. 2016;**8**(10). [PubMed: 27706049]. [PubMed Central: PMC5086648]. https://doi.org/10.3390/toxins8100288.
42. Banerjee A, Lee A, Campbell E, Mackinnon R. Structure of a pore-blocking toxin in complex with a eukaryotic voltage-dependent K(+) channel. *Elife*. 2013;**2**. e00594. [PubMed: 23705070]. [PubMed Central: PMC3660741]. https://doi.org/10.7554/eLife.00594.
43. Pardo-Lopez L, Zhang M, Liu J, Jiang M, Possani LD, Tseng GN. Mapping the binding site of a human ether-a-go-go-related gene-specific peptide toxin (ErgTx) to the channel's outer vestibule. *J Biol Chem*. 2002;**277**(19):16403–11. [PubMed: 11864985]. https://doi.org/10.1074/jbc.M200460200.
44. Lenaeus MJ, Burdette D, Wagner T, Focia PJ, Gross A. Structures of KcsA in complex with symmetrical quaternary ammonium compounds reveal a hydrophobic binding site. *Biochemistry*. 2014;**53**(32):5365–73. [PubMed: 25093676]. [PubMed Central: PMC4139162]. https://doi.org/10.1021/bi500525s.
45. Lange A, Giller K, Hornig S, Martin-Eauclaire MF, Pongs O, Becker S, et al. Toxin-induced conformational changes in a potassium channel revealed by solid-state NMR. *Nature*. 2006;**440**(7086):959–62. [PubMed: 16612389]. https://doi.org/10.1038/nature04649.
46. Yin SJ, Jiang L, Yi H, Han S, Yang DW, Liu ML, et al. Different residues in channel turret determining the selectivity of ADWX-1 inhibitor peptide between Kv1.1 and Kv1.3 channels. *J Proteome Res*. 2008;**7**(11):4890–7. [PubMed: 18937510]. https://doi.org/10.1021/pr800494a.
47. Zhao Y, Chen Z, Cao Z, Li W, Wu Y. Diverse Structural Features of Potassium Channels Characterized by Scorpion Toxins as Molecular Probes. *Molecules*. 2019;**24**(11). [PubMed: 31146335]. [PubMed Central: PMC6600638]. https://doi.org/10.3390/molecules24112045.
48. Yi H, Qiu S, Cao Z, Wu Y, Li W. Molecular basis of inhibitory peptide maurotoxin recognizing Kv1.2 channel explored by ZDOCK and molecular dynamic simulations. *Proteins*. 2008;**70**(3):844–54. [PubMed: 17729277]. https://doi.org/10.1002/prot.21706.
49. Han S, Yi H, Yin SJ, Chen ZY, Liu H, Cao ZJ, et al. Structural basis of a potent peptide inhibitor designed for Kv1.3 channel, a therapeutic target of autoimmune disease. *J Biol Chem*. 2008;**283**(27):19058–65. [PubMed: 18480054]. https://doi.org/10.1074/jbc.M802054200.